

DOCTORAL DISSERTATION

学位論文要旨

CHARACTERIZATION AND OPTIMIZATION OF
AVALANCHE PHOTODIODES FABRICATED BY
STANDARD CMOS PROCESS FOR HIGH-SPEED
PHOTORECEIVERS

高速光レシーバの実現に向けた CMOS アバランシェ光検
出器の特性評価と最適化

Optical and Electronic Sensing Laboratory

Division of Electrical Engineering and Computer Science

Graduate School of Natural Science & Technology

Kanazawa University

Student ID Number : 1424042003
Name : Zul Atfyi Fauzan Bin Mohammed Napiah
Chief Advisor : Prof. Koichi Iiyama
Date of Submission : January 2017

TABLE OF CONTENTS

ACKNOWLEDGMENT.....	iii
ABSTRACT	iv
LIST OF FIGURES.....	vi
LIST OF TABLES	ix
ABBREVIATION.....	x
CHAPTER 1: INTRODUCTION.....	1
1.1 Motivation	1
1.2 State-of-the-art.....	3
1.3 Objectives	4
1.4 Thesis Outline.....	4
1.5 Main Contribution	5
CHAPTER 2: PHOTODETECTOR.....	7
2.1 Introduction	7
2.2 Photodiode Principle	7
2.2.1 Photodetection.....	7
2.2.2 Absorption Coefficient.....	11
2.2.3 Quantum Efficiency and Responsivity	13
2.2.4 Response Speed.....	15
2.3 Avalanche Photodiode Principle.....	19
2.3.1 Avalanche Amplification	19
2.3.2 Ionization Rate	21
2.3.3 DC Characteristics.....	22
2.3.4 AC Characteristics.....	24
2.4 Summary.....	26
CHAPTER 3: AVALANCHE PHOTODIODE.....	28
3.1 Introduction	28
3.2 Characterization of CMOS-APD	29
3.2.1 Structure	29
3.2.2 Measurement System	33
3.2.3 I-V Characteristics.....	33
3.2.4 Responsivity	35
3.2.5 Frequency Response.....	36
3.3 Optimization of CMOS-APD	38
3.3.1 Electrode Spacing.....	39
3.3.2 Detection Area.....	43
3.3.3 PAD Size	44
3.3.4 The Optimum Size	45
3.4 Wavelength Dependence.....	49
3.4.1 I-V Characteristics.....	50
3.4.2 Responsivity	51
3.4.3 Frequency Response.....	53
3.5 Summary.....	56
CHAPTER 4: PHOTORECEIVER.....	57
4.1 Introduction	57
4.2 TIA.....	58
4.3 Common-Source TIA.....	59

4.3.1 Principle.....	59
4.3.2 Circuit Configuration	61
4.3.3 Simulation Results	61
4.4 Regulated-Cascode TIA	63
4.4.1 Principle	63
4.4.2 Circuit Configuration	65
4.4.3 Simulation Results	65
4.5 Summary.....	67
CHAPTER 5: CONCLUSION AND SUGGESTION	68
5.1 Conclusion.....	68
5.2 Suggestion	70
PUBLICATION	71
BIBLIOGRAPHY	72

ACKNOWLEDGMENT

I wish to express sincere appreciation and heartfelt gratitude to Professor Koichi Iiyama for the supervision, guidance, encouragement and advice throughout my study in Kanazawa University for these three and a half years. In addition, special thanks to Associate Professor Takeo Maruyama and Professor Akio Kitagawa whose familiarity with the needs and ideas of the class was helpful during the early programming phase of this undertaking. Thanks also to all ex and current lab members of the Optical and Electronic Sensing Laboratory and also my previous lab members at High-speed Laboratory for their valuable input and assistance in the preparation of this dissertation.

I also wish to express my deepest appreciation to my beloved parents; Mohammed Napiah and Zaleha, and also my beloved wife, Nurshida and my daughters, Nur Aisyi Soffyia and Aaira Nadhirah for their unconditional love, continuous prayer, patience, support, and encouragement recently and for sharing all good times and hard times throughout my academic life. Appreciation and gratitude are extending to my siblings for their continuous prayer, support, and encouragement even though they live far from me. Thanks are also due to all Malaysian students in Kanazawa and all friends for their friendship and hospitality.

Finally, my presence here to undertake this research work was made possible due to generous financial assistance from Ministry of Higher Education (MoHE) of Malaysia and Universiti Teknikal Malaysia Melaka (UTeM), to which I belong. I acknowledge with gratitude, the financial assistance from these two institutions.

ABSTRACT

A dissertation presented on the characterization and optimization of avalanche photodiodes fabricated by standard CMOS process (CMOS-APD) for high-speed photoreceivers, beginning with the theory and principle related to photodetector and avalanche photodiodes, followed by characterization, optimization, and wavelength dependence of CMOS-APD, and finally link up with the transimpedance amplifier. nMOS-type and pMOS-type silicon avalanche photodiodes were fabricated by standard 0.18 μm CMOS process, and the current-voltage characteristic and the frequency response of the CMOS-APDs with and without the guard ring structure were measured. CMOS-APDs have features of high avalanche gain below 10 V, wide bandwidth over 5 GHz, and easy integration with electronic circuits. In CMOS-APDs, guard ring structure is introduced for high-speed operation with the role of elimination the slow photo-generated carriers in a deep layer and a substrate. The bandwidth of the CMOS-APD is enhanced with the guard ring structure at a sacrifice of the responsivity. Based on comparison of nMOS-type and pMOS-type APDs, the nMOS-type APD is more suitable for high-speed operation. The bandwidth is enhanced with decreasing the spacing of interdigital electrodes due to decreased carrier transit time and with decreasing the detection area and the PAD size for RF probing due to decreased device capacitance. Thus, an nMOS-type APD with the electrode spacing of 0.84 μm , the detection area of 10 x 10 μm^2 , the PAD size for RF probing of 30 x 30 μm^2 along with the guard ring structure was fabricated. As a results, the maximum bandwidth of 8.4 GHz at the avalanche gain of about 10 and the gain-bandwidth product of 280 GHz were achieved. Furthermore, the wavelength dependence of the responsivity and the bandwidth of the CMOS-APDs with and without the guard ring structure also revealed. At a wavelength of 520 nm or less, there is no difference in the responsivity and the frequency response because all the illuminated light is absorbed in the p^+ -layer and the Nwell due to strong light absorption of Si. On the other hand, a part of the incident light is absorbed in the P-substrate and the photo-generated carriers in the P-substrate are eliminated by the guard ring structure for the wavelength longer than 520 nm, and then bandwidth

was remarkably enhanced at the sacrifice of the responsivity. In addition, to achieve high-speed photoreceivers, two types of TIA which are common-source and regulated-cascode TIAs were simulated by utilizing the output of the CMOS-APDs. The figure of merits of gain-bandwidth product was used to find the ideal results of the transimpedance gain and bandwidth performance due to trade-offs between both of them. The common-source TIA produced the transimpedance gain of 22.17 dB Ω , the bandwidth of 21.21 GHz and the gain-bandwidth product of 470.23 THz \times dB Ω . Besides that, the simulated results of the regulated-cascode TIA configuration demonstrate 79.45 dB Ω transimpedance gain, 10.64 GHz bandwidth, and 845.35 THz \times dB Ω gain-bandwidth product. Both of these TIA results meet the target of this research and further encouraging this successful CMOS-APDs to realize high-speed photoreceivers.

LIST OF FIGURES

<i>Figure</i>	<i>Page</i>
2.1 Generation of electron-hole pairs by light absorption (Intrinsic band-to-band absorption)	8
2.2 Absorption mechanism; (a) Free carrier absorption, and, (b) Band-to-impurity absorption	9
2.3 Light absorption in pn junction	11
2.4 Dark current and photocurrent	11
2.5 Incident optical power distribution in semiconductor	13
2.6 Basic equivalent circuit of photodetector. (a) actual circuit, (b) equivalent circuit, and (c) simplified circuit	16
2.7 Carrier drift in depletion layer	18
2.8 Band diagram for avalanche mechanism	21
2.9 Photocurrent - incident optical power characteristics of APD	23
2.10 Carrier movement in absorption region	26
3.1 Photograph of fabricated CMOS-APD	29
3.2 Cross-sectional structure of fabricated CMOS-APDs	30
3.3 Band diagram of the nMOS-type CMOS-APD with and without GR	30
3.4 Band diagram of the pMOS-type CMOS-APD with and without GR	32
3.5 Measurement system for CMOS-APD characterization	33
3.6 Measured I-V characteristics for (a) nMOS-type and (b) pMOS-type CMOS APDs with and without the GR	35
3.7 The responsivity of nMOS-type and pMOS-type CMOS-APDs with and without the GR as a function of the bias voltage	36
3.8 Frequency response for (a) nMOS-type and (b) pMOS-type CMOS-APD	37
3.9 The comparison of the frequency response between nMOS-type and pMOS-type CMOS-APDs with the GR	38

3.10 The relation between the avalanche gain and the bandwidth of the CMOS-APDs	
for different electrode spacing L_s	40
3.11 The relation between the responsivity and the bandwidth of the CMOS-APDs	
for different electrode spacing L_s	41
3.12 The relation between the inverse of the maximum bandwidth and the electrode	
spacing L_s	42
3.13 The device capacitance of the CMOS-APDs at 8.5 V bias voltage against the electrode spacing L_s	43
3.14 The relation between the avalanche gain and the bandwidth for different detection area S_{DT}	44
3.15 The relation between the avalanche gain and the bandwidth for different PAD	
size S_{PAD}	45
3.16 The relation between the inverse of the maximum bandwidth and the detection	
area S_{DT} and the PAD size S_{PAD}	46
3.17 The device capacitance of the CMOS-APDs at 8.5 V bias voltage against the detection area S_{DT} and the PAD size S_{PAD}	47
3.18 The relation between the device capacitance and the inverse of the maximum bandwidth	48
3.19 The relation between the avalanche gain, the responsivity and the bandwidth for the optimum nMOS-type CMOS-APD with the guard ring.....	49
3.20 Cross-sectional structure of a pMOS-type CMOS-APD	49
3.21 Measured I-V characteristics for different wavelengths	51
3.22 Wavelength dependence of the responsivity	52
3.23 Frequency responses for different wavelengths	55
4.1 The basic schematic of a TIA.....	58
4.2 Common-source TIA with shunt feedback	60
4.3 Schematic diagram of a common-source TIA	61
4.4 Frequency response of the common-source TIA	63
4.5 Regulated-cascode (RGC)	64

4.6 Schematic diagram of a regulated-cascode TIA	65
4.7 Frequency response of a regulated-cascode TIA	66

LIST OF TABLES

<i>Table</i>	<i>Page</i>
3.1 The variation size of the electrode spacing L_s , the detection area S_{DT} , and the PAD size S_{PAD} for size optimization of the fabricated CMOS-APD	39
3.2 The responsivity-bandwidth product dependence of the electrode spacing L_s	41
3.3 Estimated quantum efficiency of the CMOS-APD	53
4.1 Simulation results for selected parameters of the common-source TIA	63
4.2 Simulation results for selected parameters of the regulated-cascode TIA	66

ABBREVIATION

A - Ampere.

AC - Alternating current.

APD - Avalanche Photodiode.

CD-ROM - Compact Disc Read-Only Memory.

CMOS - Complementary Metal Oxide Semiconductor.

CR - Capacitance-Resistance.

CS - Common-source.

DC - Direct current.

DVD - Digital Versatile Disc.

FOM - Figures of merit.

FTTH - Fiber-to-the-home.

GaAs - Gallium Arsenide

GB - Gain-Bandwidth.

GR - Guard Ring.

Hz - Hertz.

InGaAs - Indium Gallium Arsenide.

InP - Indium Phosphide

I-V - Current-Voltage.

LAN - Local-area networks.

nMOS - N-type Metal Oxide Semiconductor.

PD - Photodiode.

pMOS - P-type Metal Oxide Semiconductor.

RGC - Regulated-cascode.

SML - Spatial modulated light.

TIA - Transimpedance Amplifier.

V - Voltage

VCSEL - Vertical-cavity surface-emitting lasers.

CHAPTER 1

INTRODUCTION

1.1 Motivation

Rapid emerging technology related to silicon photonics has been motivated to discover more inside its potential to be one of the most valuable findings for future development. With the advantages that exist in silicon, especially in regard to costs, it has encouraged us to make an inquiry in connection with the photoreceiver. Photoreceiver with monolithically integrated photodetectors are attractive and has a great potential of becoming one of the most important communication medium for short-distance optical data transmission for realizing local-area networks (LANs), fiber-to-the-home (FTTH) and board-to-board as well as chip-to-chip high-speed data transmissions [1]–[3]. They also can be used in optical storage systems such as Compact Disc Read-Only Memory (CD-ROM), Digital Versatile Disc (DVD) and Blue-ray Disc because it requires optical interfaces [4]–[6]. The main apparatus for all of this application is photodetector that has the capability to convert the light to electrical signal for further processing.

Although high-speed photodetectors are already commercialized mainly been implemented in III-V technology such as GaAs and InP-InGaAs for long-haul optical communication, the technology is expensive but the cost per user still low due to a large number of users. Therefore, it becomes the highest priority that a low-cost system implements in short-distance communication. This has been boost by the invention of low-cost vertical-cavity surface-emitting lasers (VCSELs) as light sources of transmitters. In order to realize the optical interconnection, it is necessary to integrate optical devices such as light sources, optical waveguides, and photodetectors with electronic circuits. By using CMOS process, it is possible to easily integrate photodetectors and electronic circuits on same Si substrate with low cost because CMOS process is a mature process.

The theory and principle behind the photodetector such as photodetection, quantum efficiency, responsivity, response speed, and etc. are needed to understand

firmly. During the penetration of incident light onto the photodetector, the photon energy has to be equal or greater than the bandgap energy to excite an electron from the valence band up into the conduction band. When a photon is absorbed, both a minority and majority carrier are generated. Inside the photodetector, both of the carriers should be separated by a depleted semiconductor region with a high electric field. This depletion region has to be thin to reduce the transit time to make sure the photodiode can operate in high-speed operation. However, the depletion layer has to be thick to increase the quantum efficiency where a large portion of the incident light can be absorbed into the photodetector. This contradiction become a trade-off between the response speed and quantum efficiency [7]. Suitable type of the photodetector is needed to fairly tackle this trade-off. In addition, despite carrier transit time, the reason that limiting the bandwidth of the photodetector is a CR time constant. Thus, the appropriate size of the photodetector devices also plays an important role to realize the high-speed response. On the other hand, the photodetector has been familiar to be characterize by using a laser of 850 nm wavelength, but, how about the other wavelength bands such as red (635 nm), green (520 nm) and blue (405 nm) visible light? Some of them are useful for photodetectors such as optical disc as mention before and etc. Therefore, the wavelength dependence of the photodetector should be conducted to further expand its applications.

Furthermore, photodetectors by themselves are generally not sufficient to be integrated with the LSI for optical information processing systems. This is because the output of the photodetector is photocurrent, while the electronic circuit at the subsequent stage is operates with the voltage signal. Additionally, in most cases, the photocurrent produced by the photodetector is quite weak. Therefore, it is essential to have an electronic circuit along with photodetector that produce the output voltage and has electronic amplification ability before it can be used for further processing. Lastly, to realize high-speed photoreceiver by using CMOS process that offer state-of-the-art performance, optimization of each device is necessary.

1.2 State of the Art

Si photodetectors fabricated by a complementary metal oxide semiconductor (CMOS) process are promising optical devices and various photodiode fabricated by CMOS process such as p-i-n photodiode [2], [8], [9], Silicon-on-insulator (SOI) photodiode PD [10]–[13], spatial modulated light detector (SML) [14]–[19] and avalanche photodiode (APD) [20]–[23] has been developed for optical interconnection applications. There are two desirable indicators to recognize a good photodiode that are consumes high detection efficiency and large bandwidth product. The p-i-n and SOI photodiodes can produce maximum bandwidth near 13 GHz but have the disadvantage of the low detection efficiency. Nevertheless, due to the light penetration depth of Si at 850 nm is more than 10 μm , another problem arises that carriers generated from the bulk Si substrate diffuse slowly and are collected, significantly affecting the response performance and limiting the bandwidth. The emergent of SML photodiodes can provide slow diffusion carriers elimination by the differential structure as reported by [14] with the highest bandwidth is about 4.4 GHz and the responsivity around 0.034 A/ μm . However, SML PDs suffer from responsivity degradation because about half of optical input power is blocked as reported by [17], and then they come out a solution by combining the speed advantage of the SML PD and the responsivity advantage of a normal PD so-called speed-enhanced PD, but, unfortunately no bandwidth and responsivity data provided.

Several researchers have implemented a different approach to eliminating the slow diffusion carriers that limiting the speed performance and prevent the lack of responsivity by designing the avalanche photodiode with CMOS compatible (CMOS-APD) [20]–[23]. Avalanche photodiode is a highly sensitive semiconductor electronic device that provide built-in gain so-called avalanche multiplication. By applying higher reverse voltage bias, APDs produce an internal gain effect due to impact ionization. This phenomenon became an advantage for APDs to have higher quantum efficiency. Besides that, guard ring structure [23]–[25] that already implemented in the avalanche photodiode enhanced the avalanche

effect and provides the maximum avalanche gain. The incorporating of guard ring also gives extra value for APDs due to ability to eliminate the slow diffusion carriers in deep layer and substrate device for higher speed generation.

1.3 Objectives

The development of integrated circuit technology in recent years is remarkable, and the processing speed improves year by year. As we know, the performance of large scale integrated, LSI has been enhanced by down-sizing the LSI. However, due to the down-sizing, resistance in electric wire is increased due to decreasing wire dimension, and capacitance between electric wires is increased due to narrow wire separation. Consequently, the operating speed of the LSI is limited. To enhance the operating speed of the LSI, optical interconnection has been proposed and widely studied. Optical interconnection has no resistance and has no capacitance. Thus, high-speed operation of the LSI is expected. To realize the optical interconnection, optical devices such as lasers, waveguides, photodetectors and LSIs should be integrated in one chip. Therefore, in this research, there have two main objectives that focus on photodetector mainly for avalanche photodiode, which are (1) to characterize and optimize the avalanche photodiodes, and (2) to study the wavelength dependence of the avalanche photodiode. In addition, to realize high-speed photoreceiver by using CMOS process, the avalanche photodiodes should be combined with the transimpedance amplifier. Hence, another objective is to investigate the transimpedance amplifier that can produce high gain and high bandwidth performance by utilizing the output from the optimum avalanche photodiode.

1.4 Thesis Outline

In this Chapter 1, the motivation, state-of-the-art, and objective to represent the whole idea for this thesis was briefly explained. This chapter also reviews the earlier photodiodes designed by other researchers and deliberate the pros and cons between them. Thereafter, the main contribution of this thesis is revealed. In Chapter 2, as the photodetector is the very first building block of the photoreceiver, it is important to review the basic principle regarding photodiodes. After that, the

selected photodetector for this research that is avalanche photodiode and its respective principle and characteristics are described.

Chapter 3 presents the characterization and optimization of the avalanche photodiode. The characterization of CMOS-APDs is treated first followed by the optimization. Several criteria have been subject to optimize the CMOS-APDs such as electrode spacing, detection area, pad size for RF probing and wavelength. All of the results and discussions are explained here.

After the discussion about avalanche photodiodes are almost complete, the photoreceiver part is deliberated in Chapter 4. In this chapter, the explanation of photoreceiver mainly transimpedance amplifier is conducted first followed by two different types of transimpedance amplifiers with their circuit configuration, principles and simulation results.

Finally, the general conclusions are drawn in Chapter 5. An overview is also given on the main contribution based on the results that have been described in the previous chapters and also in international journals which have been presented. Then, the suggestions or recommendations are made for upcoming research that could continue to improve and advance the performance of this finding.

1.5 Main Contribution

The work presented in this thesis gives the original contribution to the characterization and optimization of avalanche photodiodes which are fabricated by standard CMOS process to realize high-speed photoreceivers. For the first time, the optimization of avalanche photodiode in regards of electrode spacing, detection size, and pads size are acknowledged. The achieved 8.4 GHz bandwidth along with 280 GHz gain-bandwidth product are more than the state-of-the-art commercial PIN photodiodes. Furthermore, in this research, the wavelength dependence of the responsivity and the bandwidth of the CMOS-APDs with and without the guard ring structure shows the guard ring is very beneficial for practical application. The guard ring enhances bandwidth although the responsivity is decreased for wavelength longer than 520 nm. For wavelength shorter than 520 nm, although the

bandwidth is same regardless of with or without the guard ring, the guard ring is very effective for realizing low dark current.

To keep the amazing results of avalanche photodiodes in line with high demands of the high-speed photoreceivers, the research continued with developing the transimpedance amplifier (TIA). Two types of TIA which are common-source and regulated-cascode have been selected to perform the conversion of small photocurrent from CMOS-APD to voltage signal. The simulation results of the TIAs are very promising for high-speed photoreceivers in regard of CMOS-APDs performance.

CHAPTER 2

PHOTODETECTOR

This chapter will describe the information needed to easily understand the basic operation of photodiodes followed by the avalanche photodiodes.

After the introduction of photodetector, the principle of a photodiode such as photodetection, absorption coefficient, quantum efficiency, responsivity, response speed, and etc. are explained. Thereafter, the discussion is concentrated on avalanche photodiode which is the main photodiode for this research. It is concern to the avalanche amplification, ionization rate, multiplication factor, and frequency response. Finally, all the key points related to this chapter are summarized.

2.1 Introduction

The main component in photoreceiver's block is a photodetector. Photodetector performed the first task for the photoreceiver which is to convert from the optical signal to the electric form, mainly in current. The photodetector used in this research is a silicon CMOS photodiode, as this is the most inexpensive semiconductor used in electronics. Semiconductor photodetectors depending on the absorption of incident photons with energy more than the semiconductor bandgap energy E_g to generate electron-hole pairs. Apparently, photodetection involves three processes: (1) optical energy absorption and carrier generation, (2) the transportation of photogenerated carriers away from the absorption region, (3) carrier collection and photocurrent generation. The performance of a photodetector can be characterized by a number of figures of merit (FOM) such as responsivity and bandwidth.

2.2 Photodiode Principle

2.2.1 Photodetection

Photodetection occurs when the electrons in the valence band excited by the photon energy which is greater than the material bandgap energy E_g , and then up

into the conduction band as shown in Figure 2.1. Holes are generated because the electrons are lost from the valence band. The hole and electron each compose a charge carrier. When the electric field is applied to the semiconductor, it causes the holes and electrons to be transported through the material and into an external circuit, yielding a photocurrent. This mechanism so-called the intrinsic band-to-band absorption is the common absorption mechanism in most semiconductor used for photodetection besides free carrier absorption and band-to-impurity absorption as shown in Figure 2.2. However, when the photon energy is smaller than the material bandgap energy E_g , the electrons are not excited to the conduction band.

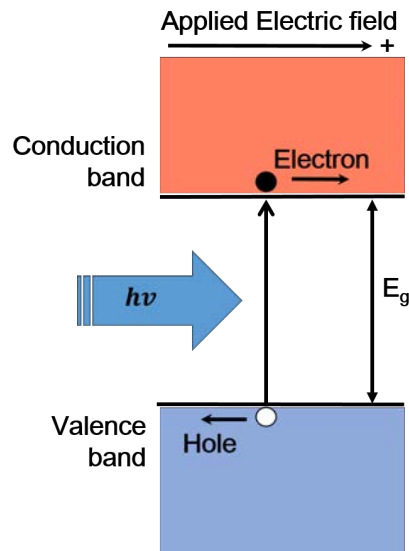


Figure 2.1: Generation of electron-hole pairs by light absorption (Intrinsic band-to-band absorption) [26].

The relationship between the photon energy, E and the wavelength of light are as below:

$$E = \frac{hc}{\lambda} \quad (2.1)$$

where,

E : photon energy

h : Planck's constant

λ : wavelength of light

c : speed of light

Equation 2.1 shows that the shorter light wavelength has stronger photon energy. In order for electrons in the valence band to be excited and transferred to the conduction band, the photon energy E must be larger than the energy bandgap E_g and the electron hole pairs are generated by the absorption of light. Therefore, excitation does not occur in an environment in which the photon energy is equal to or smaller than the bandgap E_g . Therefore, the conditions for effective excitation of electrons is as follows:

$$E = \frac{hc}{\lambda} \geq E_g \quad (2.2)$$

this yields an allowable wavelength of light

$$\lambda \leq \frac{hc}{E_g} \quad (2.3)$$

or

$$\lambda = \frac{1.24}{E_g(\text{eV})} [\mu\text{m}] \quad (2.4)$$

where:

E_g (eV) = bandgap energy in electron–volts.

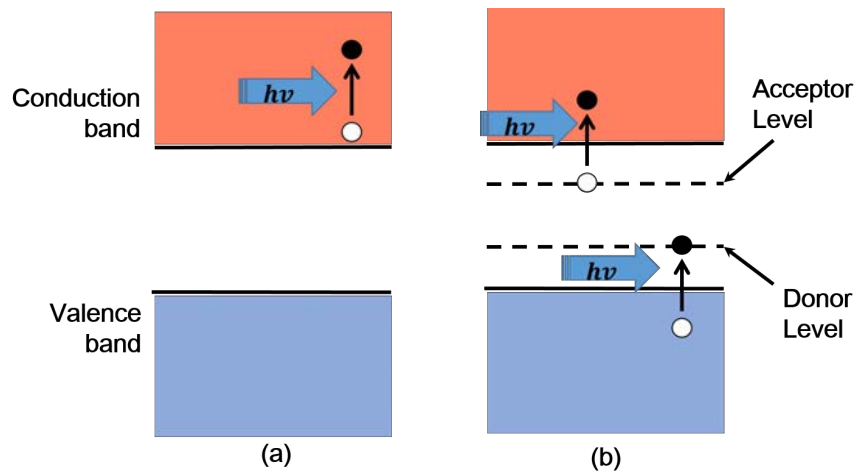


Figure 2.2: Absorption mechanism; (a) Free carrier absorption, and, (b) Band-to-impurity absorption [26].

In addition, free carrier absorption occurs when the photon energy is absorbed by free carriers in either the conduction or the valence band [26] and corresponds to the ‘heating’ of the semiconductor material. It is a secondary effect at the near infrared wavelengths used for optical communications. Band-to-impurity absorption is another secondary effect at near infra-red wavelengths. It is used to construct photodetectors responsive at mid infra-red wavelengths as long as 30 μm .

Figure 2.3 shows the band diagram near the pn junction to consider the situation when a reverse voltage V is applied to the pn junction from the outside. When semiconductor is incident with light, electron-hole pairs are generated by light absorption. At this time, the holes in the n-region, which are minority carriers, and the electrons in the p-region are minority carriers, so that those generated at a location distant from the depletion layer diffuse by the diffusion length and then disappear by recombination. On the other hand, carriers generated in the depletion layer and part of carriers generated in the diffusion length region from the depletion layer drift to the n-region and p-region for electrons and holes, respectively. The reverse current by these carriers is the photocurrent I_{ph} .

However, the dark current I_{dark} occurs when the reverse voltage is applied. It is due to the following factors:

- (i) Reverse saturation current generated by carrier diffusion,
- (ii) Surface leakage current generated from the interface state existing at the interface with air or dissimilar materials,
- (iii) Tunnel current flowing through the thin potential barrier of the depletion layer when high voltage applied,
- (iv) Current generated by lattice defects in the material.

Based on these four factors, the total current I when applying the reverse voltage is,

$$I = -(I_{ph} + I_{dark}) \quad (2.5)$$

Thus, when a certain reverse voltage V_B is applied, an avalanche breakdown phenomenon occurs where the current increases obviously. This phenomenon will be described later.

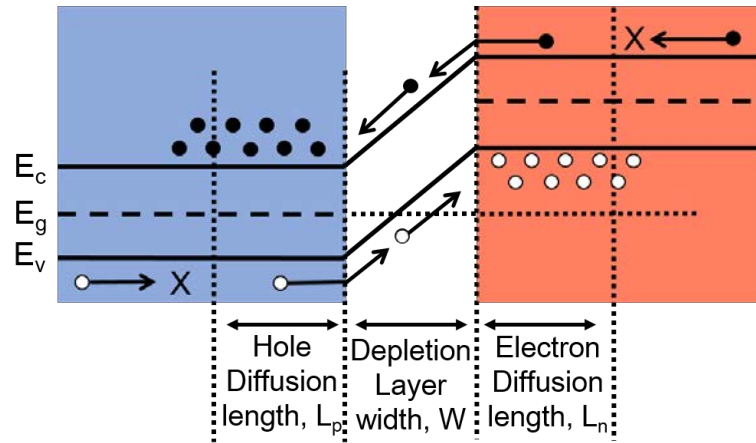


Figure 2.3: Light absorption in pn junction

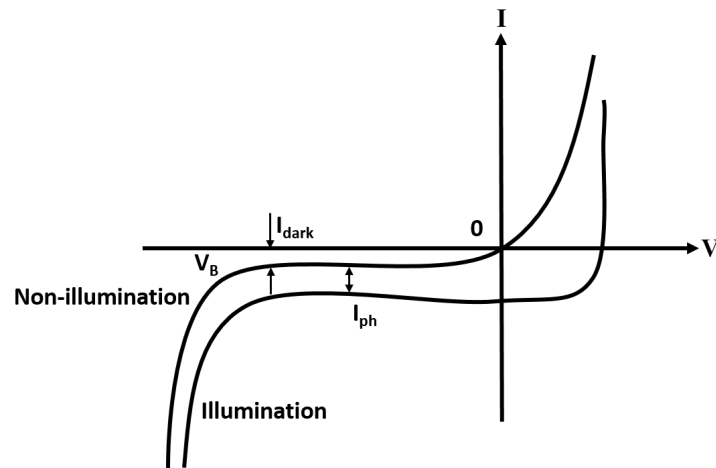


Figure 2.4: Dark current and photocurrent

2.2.2 Absorption Coefficient

As described in the previous section, if light adequate the equation (2.4) when illuminated on the material, the light absorption occurs. An absorption coefficient α_0 indicating the light absorption intensity per unit length is represent the constant for the extended light absorption. Assuming that the incident optical power at the surface is expressed as $P_i(x)$. When light is penetrated on the material, the light absorption $-dP_i(x)$ at the distance dx is expressed as follows:

$$\begin{aligned}
-dP_i(x) &= \alpha_0 P_i(x) dx \\
\frac{-dP_i(x)}{dx} &= -\alpha_0 P_i(x)
\end{aligned} \tag{2.6}$$

By integrating both of equations in (2.6) with x after considering the initial condition $P_i(0) = P_{i0}$, it become:

$$P_i(x) = P_{i0} e^{-\alpha_0 x} \tag{2.7}$$

Therefore, the incident optical power distribution in the material is exponentially decreases according to the absorption coefficient α_0 . This is shown in Figure 2.5. L_α is the absorption length or the depth that light can enter into the material. Assuming that the incident optical power P_{i0} on the material surface is absorbed into the material, the absorption length L_α from the equation (2.7) is then expressed as,

$$\begin{aligned}
P_{i0} L_\alpha &= \int_0^\infty P_{i0} e^{-\alpha_0 x} dx \\
L_\alpha &= \frac{1}{\alpha_0}
\end{aligned} \tag{2.8}$$

So, L_α becomes the reciprocal of the absorption coefficient α_0 . The incident optical power at the absorption length is expressed as,

$$P_i(L_\alpha) = P_{i0} e^{-\alpha_0 L_\alpha} = \frac{1}{e} P_{i0} \cong 0.37 P_{i0} \tag{2.9}$$

Therefore, it decreases about 37% of the incident optical power at the surface. In other words, 63% of light is absorbed to the absorption length. Since the absorption coefficient is generally 10^2 to 10^5 cm^{-1} , the absorption length is 0.1 to 100 μm . Therefore, it is understood that most of light is absorbed in a very shallow material surface.